Electronic Supplementary Material (ESI) for Materials Advances.

NiGraf: A new nickel-based molecularly doped metal for enhanced water electrolysis

Mario Pagliaro,[a*] **Maria V. Pagliaro**,[b] **Rocco Caliandro**,[c] **Cinzia Giannini**,[c*]
Rosaria Ciriminna,[a*] **Alessandro Lavacchi**[b*]

[a]*Istituto per lo Studio dei Materiali Nanostrutturati, CNR, via U. La Malfa 153, 90146 Palermo, Italy;* [b]*Istituto di Chimica dei Composti Organometallici, CNR, via Madonna del Piano 10, 50019 Sesto Fiorentino FI, Italy;* [c]*Istituto di Cristallografia, CNR, via G. Amendola 1220, 70126 Bari, Italy*

Electronic Supplementary Information

1. Determination of the crystal phase composition

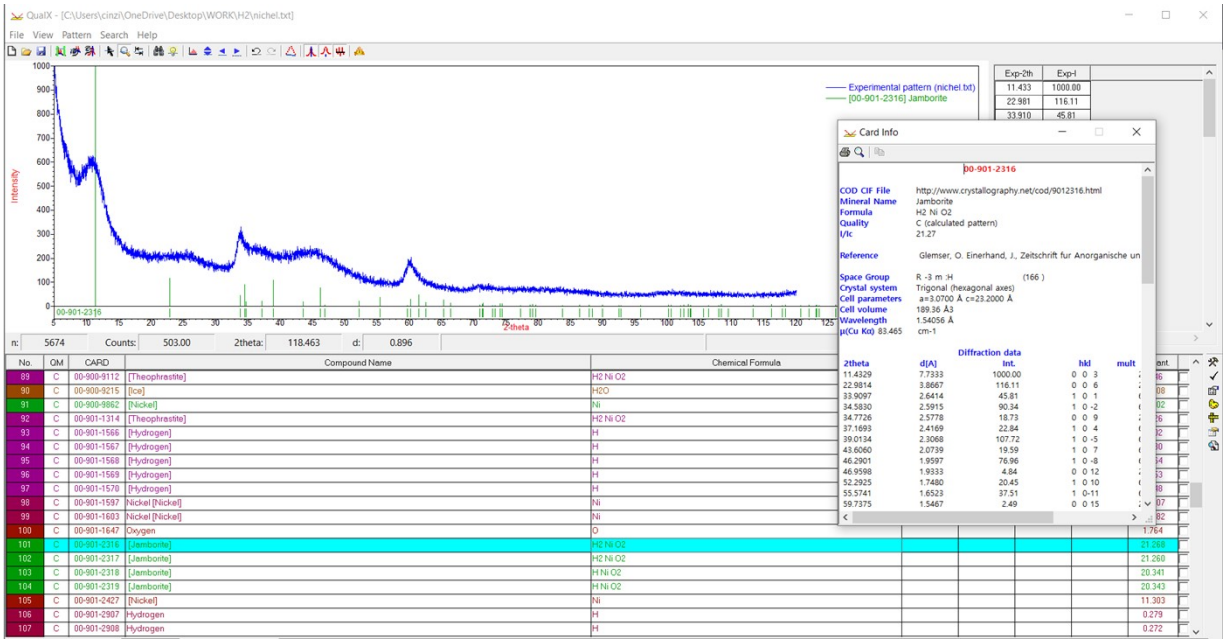

Figure S1. Screenshot of the QUALX [https://www.ic.cnr.it/software/qualx/] graphic output, showing the identification of jamborite as the most probable crystal phase present in the lab XRD profile of the NG1 sample.

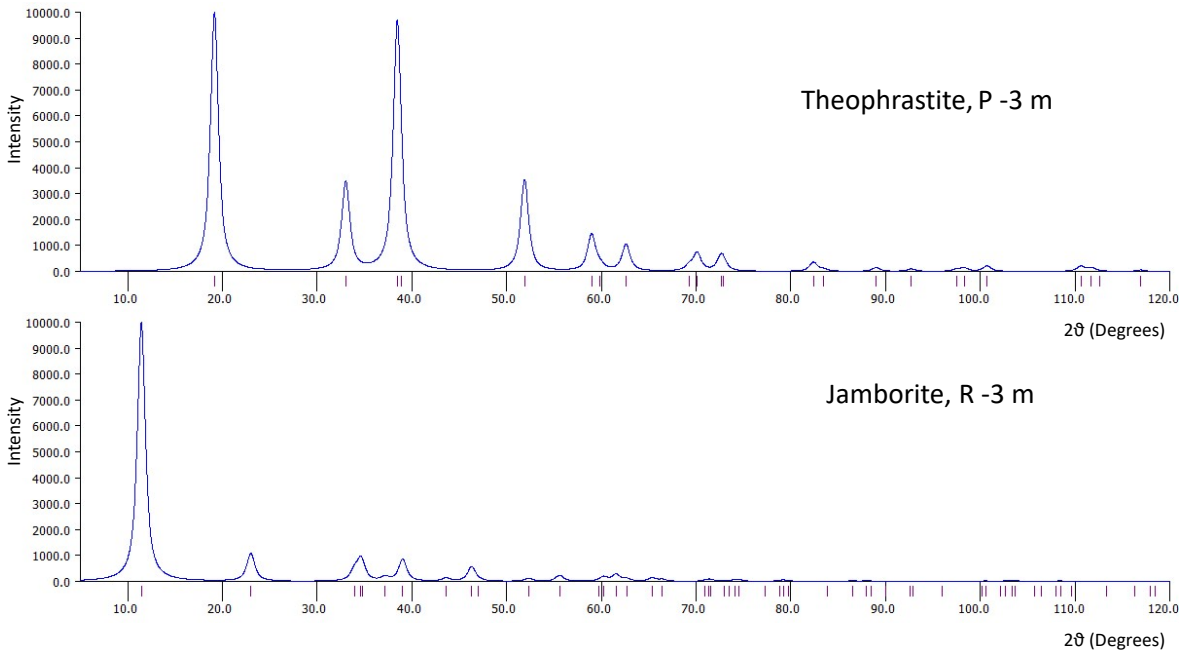

Figure S2. XRD profiles calculated from two $Ni(OH)_2$ polymorphs: theophrastite (top) and jamborite (bottom).

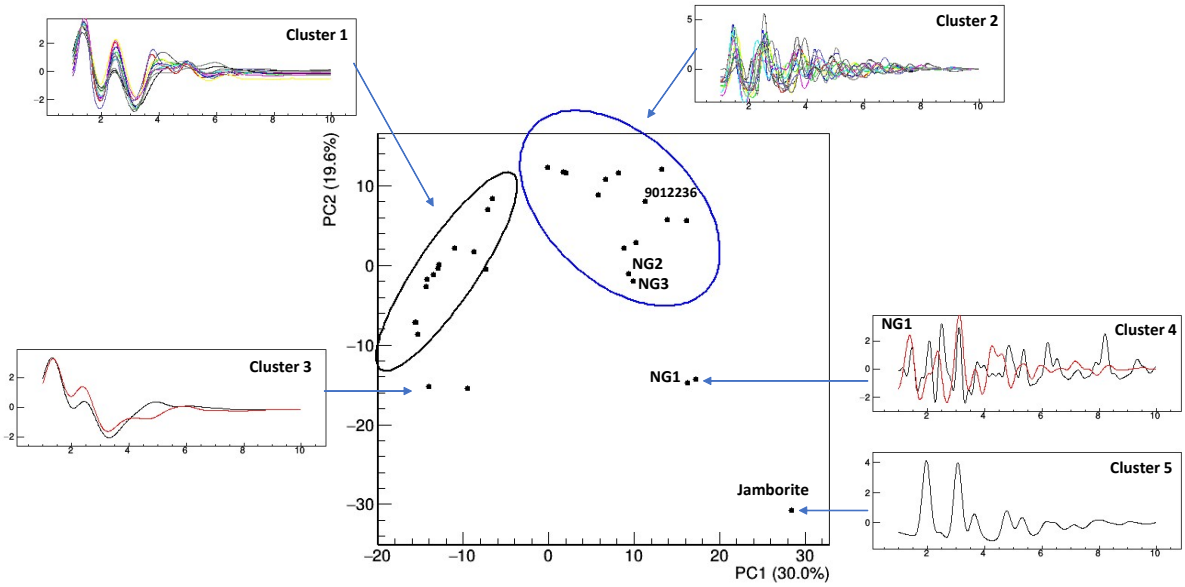

Figure S3. PCA-assisted identification of the crystal phase composition of the NG samples, based on the PDF profiles (reported in the insets). The experimental PDF profiles of NG1, NG2 and NG3 and those calculated from the crystal structures reported in Table S1 are represented by a data point in the score plot of the first two PCA components, PC1 and PC2. Their variance percentages explained are reported on the corresponding axes. The data points are clustered according to their position in the score plot and PDF profiles of the same cluster are superposed in the insets.

Table S1. Composition of the clusters shown in Figure S1 and images of the crystal structures used to calculate the PDF profiles. The crystal structures are identified by their COD or CCDC numbers.

Cluster 1	**Cluster 2**	**Cluster 3**	**Cluster 4**	**Cluster 5**
COD 1543272 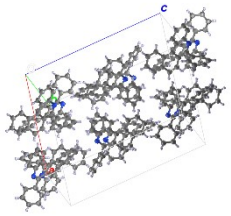	NG2	COD 4002026 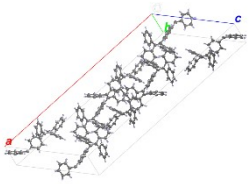	NG1	COD 9012317 (Jamborite) 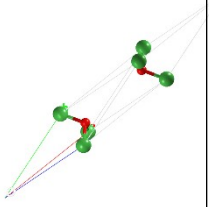
COD 4002025 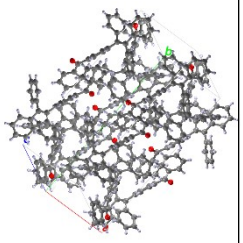	NG3	COD 7235236 planar fragment 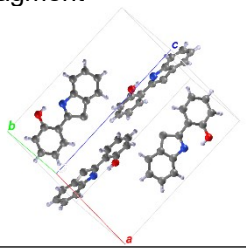	COD 9012241 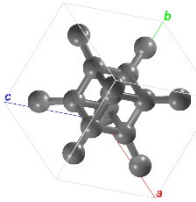	
COD 4120862	COD 9000046			

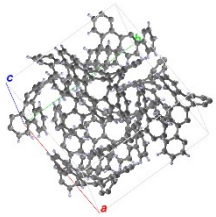	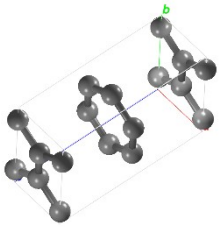			
COD 4119215 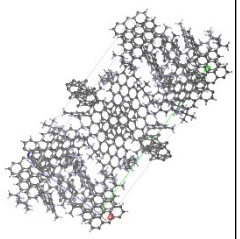	COD 9011577 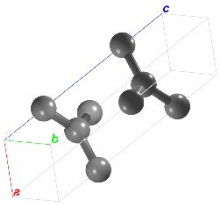			
COD 4119216 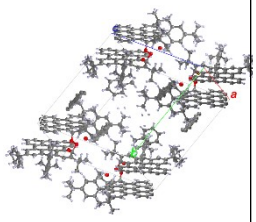	COD 9012232 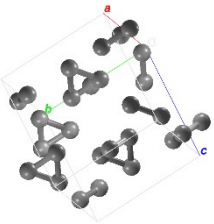			
COD 4123602 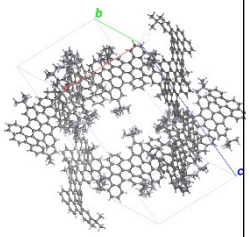	COD 9012234 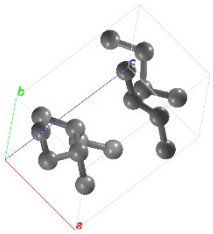			
COD 7116967 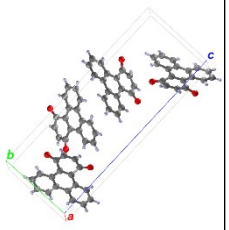	COD 9012235 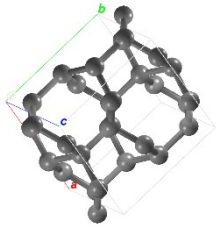			
COD 7116968 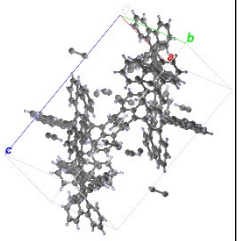	COD 9012236 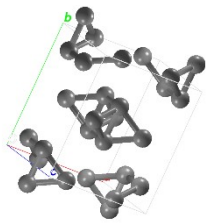			
COD 7116969	COD 9012237			

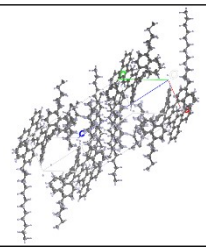	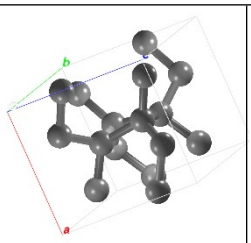			
COD 7116971 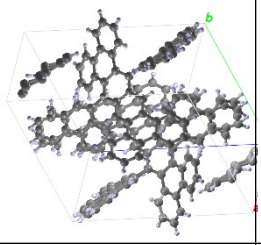	COD 9012238 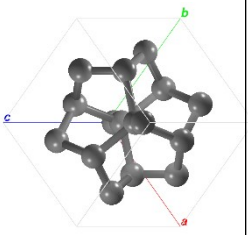			
COD 7235236 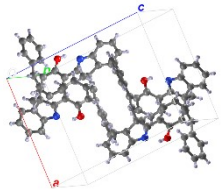	COD 9012239 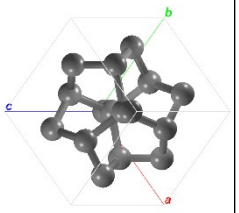			
CCDC 2003039 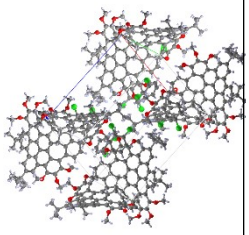	COD 9012243 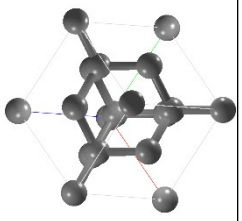			
	COD 9012230 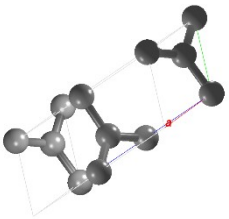			
	COD 9012705 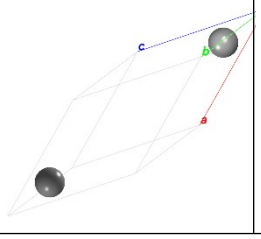			

2. Structural refinement

Table S2. Parameters determined by fitting of the PDF profiles of the NG1, NG2 and NG3 samples with a structural model composed by a linear superposition between the crystal structures COD 9012317 (jamborite) and COD 9012236 (GO). R_w is the weighted agreement factor between observed and calculated PDF, Q_{broad} describes the peak broadening from increased intensity noise at high Q, *Scale* is the parameter that weights the amount of jamborite in the linear superposition between the two crystal structures, δ_1 is the coefficient for 1/r contribution to the peak sharpening, $SP_{diameter}$ is the particle diameter for the PDF shape damping function. The parameters Q_{broad} *and* δ_1 have not be introduced for the fit of NG2 and NG3, since they are only significant for refinements over wider *r* ranges.

	NG1	**NG2**	**NG3**
Fit range	1-20 Å	1-15 Å	1-15 Å
R_w	0.399	0.360	0.370
Q_{broad}	0.25		
COD 9012317 Jamborite (R -3m)			
Scale	0.215	0.015	0.025
δ_1	2.45		
Cell parameters	a=b=c=9.14 Å α=β=γ=19.5°	a=b=c=9.05 Å α=β=γ=19.6°	a=b=c=9.30 Å α=β=γ=19.1°
COD 9012236 GO (C mmm)			
$SP_{diameter}$	6.6 Å	9.9 Å	10.5 Å
Cell parameters	a=5.02 Å, b=5.66 Å, c=4.19 Å	a=4.91 Å, b=7.17 Å, c=4.13 Å	a=4.91 Å, b=7.17 Å, c=4.11 Å

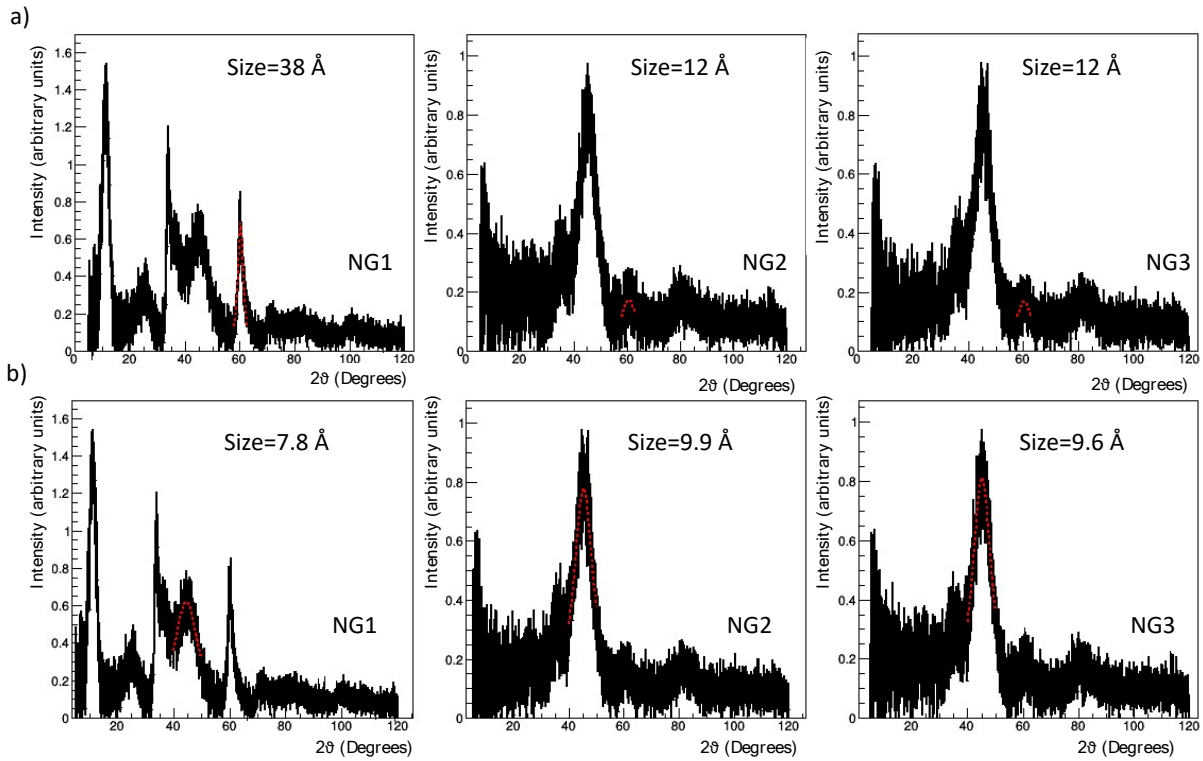

Figure S4. Average size determined by the lab XPD profiles by considering the common peak at 2θ = 60.4°, assigned to the jamborite phase (a) and at 2θ = 45°, assigned to the GO phase (b). Background subtracted profiles (black lines) are fitted by PseudoVoigt function (dashed red lines).

3. Electrochemical supporting data

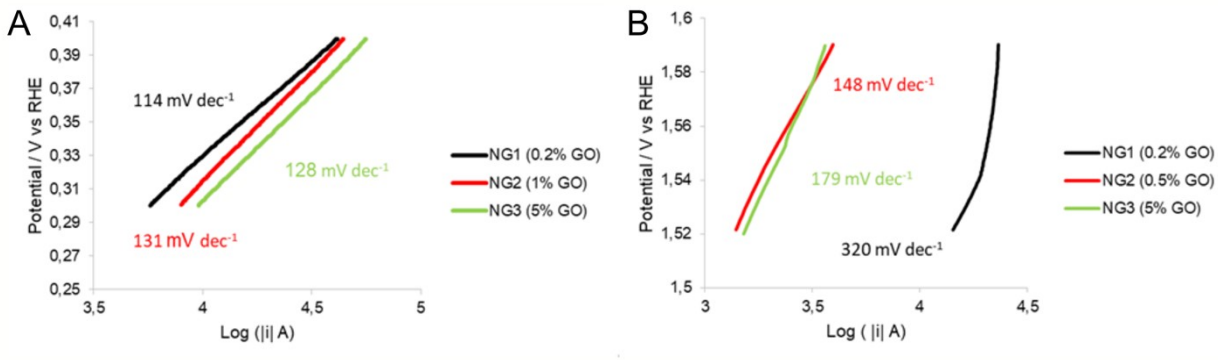

Figure S5. A) HER and B) OER Tafel curves and slope values extrapolated from linear fitting of respective LSV curves.

HER and OER Tafel plots and extrapolated Tafel slope values are reported in Figure S5. For HER, NG1, NG2, and NG3 show all similar values around 120 mV dec^{-1} between -0.3 and -0.4 V *vs.* RHE, indicating that the HER occurs through the same Volmer-Heyrovsky mechanism. The Tafel values for OER, calculated between 1.5 and 1.6 V, are higher than 120 mV dec^{-1} and compatible with the presence of oxidized species, but these values do not provide specific indications on the type of mechanism for the oxygen evolution reaction.

The electrochemical impedance spectroscopy (EIS) measurements were acquired at constant applied potentials, -0.3 V *vs.* RHE for HER, and 1.6 V *vs.* RHE for OER. The measurements were acquired in N_2 purged KOH 0.1 M. The respective Nyquist plots are shown in Figure S6 A) and B).

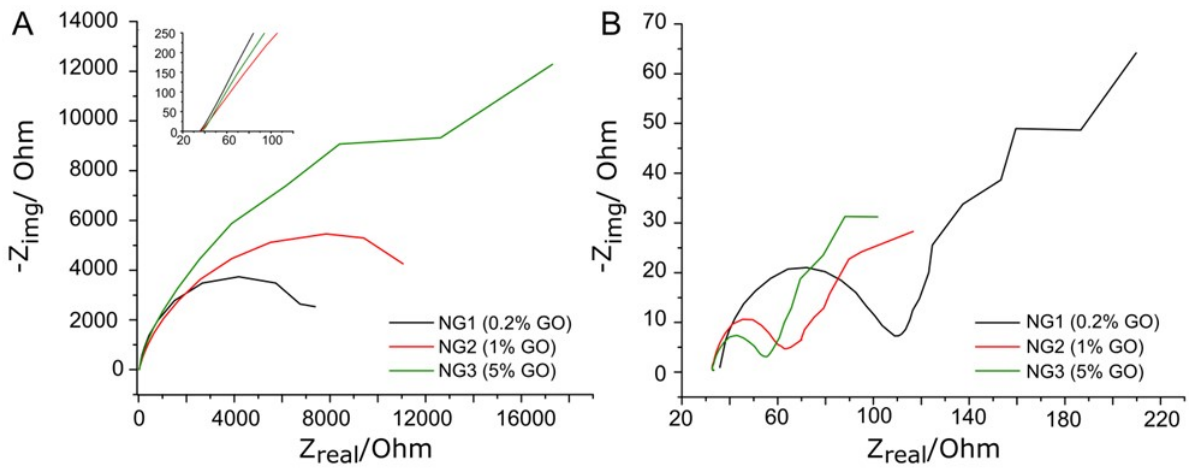

Figure S6 Nyquist plot of the three samples NG1-2-3: A) for HER at -0.3 V *vs.* RHE and 1600 rpm, B) for OER at 1.6 V *vs.* RHE and 1600 rpm.

The EIS results show that OER is a more favorable reaction on the surface of NiGraf catalysts than HER and highlight a different trend for catalysts. The three NG NiGraf samples exhibited in general lower charge transfer resistance for OER, with growing R_{CT} values in the order NG3>NG2>NG1 as expected, confirming that NG3 is the most active catalyst. Moreover, NG2 and NG3 samples exhibit similar C_{dl} values, one order of magnitude larger with respect to NG1 (Table S3). EIS results for HER demonstrate that this reaction is more sluggish with respect to OER, with substantially higher R_{CT} values, especially for the NG3 sample with the highest GO content.

Table S3. EIS extrapolated data through fitting with a simple Randles circuit modified with a Warburg diffusion element.

Sample	HER (-0.3 V *vs.* RHE)		OER (1.6 V *vs.* RHE)	
	R_{CT} (Ω)	C_{dl} (μF)	R_{CT} (Ω)	C_{dl} (μF)
NG1	77	272	68	0.9
NG2	586	141	30	12
NG3	1300	150	18	15

4. Scanning Electron Microscopy (SEM)

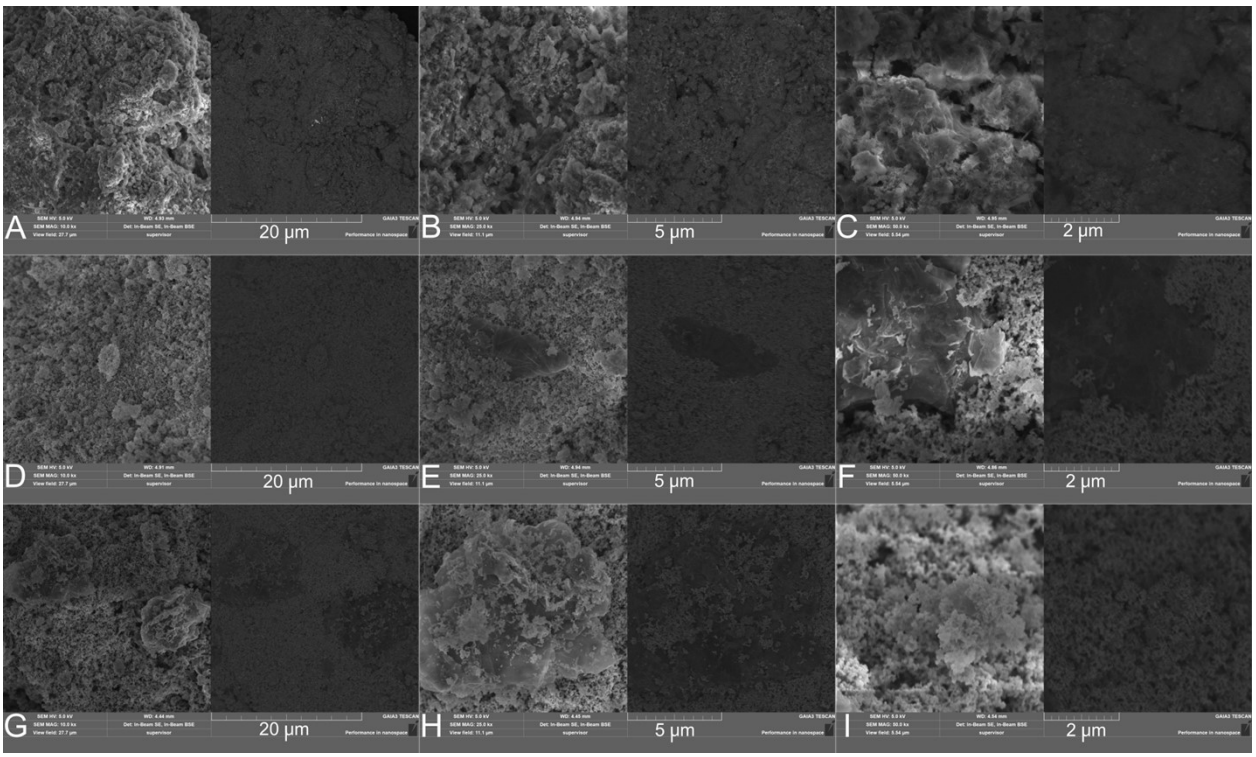

Figure S7. SEM images of NG1 (0.2% GO): (A): low magnification (×10k), (B,C): high magnification (×25k and ×50k). SEM images of NG2 (1% GO): (D): low magnification (×10k), (E,F): high magnification (×25k and ×50k). SEM images of NG3 (5% GO): (G): low magnification (×10k), (H,I): high magnification (×25k and ×50k).